Published in final edited form as:

Am J Transplant. 2016 October ; 16(10): 3016–3023. doi:10.1111/ajt.13907.

Noninvasive Imaging of CCR2+ Cells in Ischemia Reperfusion Injury after Lung Transplantation

Yongjian Liu[1,*], **Wenjun Li**[2], **Hannah P. Luehmann**[1], **Yongfeng Zhao**[1,^], **Lisa Detering**[1], **Deborah E. Sultan**[1], **Hsi-Min Hsiao**[2], **Alexander S. Krupnick**[2,3], **Andrew E. Gelman**[2,3], **Christophe Combadiere**[4], **Robert J. Gropler**[1], **Steven L. Brody**[1,5], and **Daniel Kreisel**[2,3,*]

[1]Department of Radiology, Washington University School of Medicine, St. Louis, MO, USA

[2]Department of Surgery, Washington University School of Medicine, St. Louis, MO, USA

[3]Department of Pathology & Immunology, Washington University School of Medicine, St. Louis, MO, USA

[4]Sorbonne Universités, UPMC Univ Paris 06, INSERM, U1135, CNRS, ERL 8255, Centre d'Immunologie et des Maladies Infectieuses (CIMI-Paris), 91 Boulevard de l'Hôpital, F-75013 Paris, France

[5]Department of Medicine, Washington University School of Medicine, St. Louis, MO, USA

Abstract

Ischemia reperfusion injury-mediated primary graft dysfunction substantially hampers short- and long-term outcomes after lung transplantation. This condition continues to be diagnosed based on oxygen exchange parameters as well as radiological appearance, and therapeutic strategies are mostly supportive in nature. Identifying patients who may benefit from targeted therapy would therefore be highly desirable. Here, we show that CCR2 expression in murine lung transplant recipients promotes monocyte infiltration into pulmonary grafts and mediates graft dysfunction. We have developed new positron emission tomography imaging agents using a CCR2 binding peptide ECLi1 that can be used to monitor inflammatory responses after organ transplantation. Both ^{64}Cu-radiolabeled ECL1i peptide radiotracer (^{64}Cu-DOTA-ECL1i) and ECL1i-conjugated gold nanoclusters doped with ^{64}Cu (^{64}CuAuNCs-ECL1i) showed specific detection of CCR2, which is up-regulated during ischemia-reperfusion injury after lung transplantation. Due to its fast pharmacokinetics ^{64}Cu-DOTA-ECL1i functioned efficiently for rapid and serial imaging of CCR2. The multivalent ^{64}CuAuNCs-ECL1i with extended pharmacokinetics is favored for long-term CCR2 detection and potential targeted theranostics. This imaging may be applicable for diagnostic and therapeutic purposes for many immune-mediated diseases.

[*]Correspondence to: Yongjian Liu, Ph.D., Assistant Professor of Radiology, 510 S. Kingshighway Blvd, Campus Box 8225, Washington University School of Medicine, St. Louis, MO 63110, Tel: (314) 362-8431, Fax: (314) 362-9940, yongjianliu@wustl.edu or Daniel Kreisel, M.D., Ph.D., Professor of Surgery, Pathology & Immunology, Campus Box 8234, 660 South Euclid Avenue, Washington University School of Medicine, St. Louis, MO 63110, Tel: (314) 362-6021, Fax: (314) 367-8459, kreiseld@wudosis.wustl.edu.

[^]Y. Z. is currently at Jackson State University, Jackson, MS.

Disclosure

The authors of this manuscript have no conflicts of interest to disclose as described by the American Journal of Transplantation.

Supporting Information

Additional Supporting Information may be found in the online version of this article.

Introduction

Ischemia reperfusion injury-mediated primary graft dysfunction is a critically important contributor to early and late morbidity as well as mortality after lung transplantation (1). The incidence of primary graft dysfunction after pulmonary transplantation has not changed substantially over the last few decades. Up to 80% of lung transplant recipients experience some degree of primary graft dysfunction based on broad clinical criteria (2). These include non-specific features, such as impaired oxygen exchange and pulmonary infiltrates on chest radiographs. Likewise, the treatment for these patients has been mainly supportive. Therefore, developing novel diagnostics and therapeutics for this condition and identifying patients who could benefit from targeted strategies would be desirable.

Recruitment of innate immune cells to lungs shortly after reperfusion plays a key role in mediating tissue injury. We have reported that in addition to their well-recognized role in promoting acute injury, neutrophils can enhance adaptive immune responses after pulmonary transplantation (3). We have demonstrated that monocytes facilitate the extravasation of neutrophils into reperfused lungs indicating that for pulmonary graft dysfunction, monocytes play a critical role in orchestrating tissue injury (4). These observations may be more generalizable as $CCR2^{+}$ monocytes promote the transendothelial migration of neutrophils in murine models of arthritis (5). Mouse monocytes are heterogeneous with $CD11b^{+}Ly6C^{high}CCR2^{high}$ monocytes considered to be an inflammatory subset. Experiments using CCR2-deficient mice have demonstrated that CCR2 signaling contributes to myocardial, renal and cerebral ischemia reperfusion injury (6–8). Attenuation of injury was associated with reductions of monocytic and neutrophilic infiltration into the affected tissues.

Several CCR2 antagonists including small molecules and antibodies have been used as inhibitors in various inflammatory diseases, experimentally and clinically (9). However, clinical trials have yielded equivocal or negative results (10, 11). This may be due to recruitment of anti-inflammatory monocyte populations or other chemokine receptors contributing to inflammation. Moreover, inadequate dosing or duration of therapy due to concerns for toxicity or impedance of the essential role of CCR2 for immune surveillance may cloud the benefit of antagonists. It would therefore be desirable to devise a non-invasive CCR2 imaging technique, which is not only able to monitor the degree of receptor occupancy to aid in dose selection, but also to determine the therapeutic response in real time (12).

Here we report the use of CCR2-specific molecular probes through the conjugation of a novel targeting peptide for positron emission tomography (PET) imaging in a mouse model of lung transplant-mediated ischemia reperfusion injury. This work may provide a powerful tool for the sensitive and specific detection of CCR2 to track inflammatory monocytes in various pathological conditions and lay the foundation for new approaches for the diagnosis and treatment of immune-mediated processes such as ischemia reperfusion injury and rejection in transplant recipients.

Materials and Methods

Mice and surgical procedures

C57BL/6 (B6), B6 CD45.1 and B6 CCR2-deficient mice were purchased from The Jackson Laboratories (Bar Harbor, ME) and maintained in pathogen-free facilities. Left lung transplants were performed following 1 hour of storage in low-potassium-dextran solution at 4°C unless otherwise specified (13).

PET Imaging

At 1 hour after transplantation, 0–60 min dynamic PET/CT scan was performed following injection of ^{64}Cu-DOTA-ECL1i (100 μCi in 100 μL saline) with microPET Focus 220 (Siemens, Malvern, PA) or Inveon PET/CT system (Siemens, Malvern, PA) (Figure S1). For PET/CT imaging at 4 and 24 hours after transplantation, a 30-minute background scan (10 min/frame, 3 frames) was performed prior to injecting ^{64}Cu-DOTA-ECL1i (100 μCi in 100 μL saline). The *in vivo* retention of ^{64}Cu-DOTA-ECL1i in the donor lung from the previous injection was quantified and subtracted from the uptake value at 4 or 24 hours (Figure S2). For ^{64}CuAuNCs-ECL1i, PET/CT was conducted 1 hour after transplantation. A static scan was performed at 1, 4 and 24 hours after injection. The PET images were reconstructed with the maximum a posteriori algorithm and analyzed by Inveon Research Workplace. The organ uptake was calculated as percent injected dose per gram (%ID/g) of tissue in three-dimensional regions of interest without correction for partial volume effect (14). Competitive PET blocking studies were performed immediately after transplantation with co-injection of non-radiolabeled ECL1i and ^{64}Cu-DOTA-ECL1i (ECL1i: ^{64}Cu-DOTA-ECL1i molar ratio = 500:1) followed by a 0–60 minute dynamic scan. ^{18}F-FDG (250 μCi in 100 μL saline) PET/CT was performed following the same protocol as ^{64}Cu-DOTA-ECL1i (15). To measure surgery-induced blood flow changes in lungs, ^{15}O-water (~1 mCi) was injected intravenously into mice used for ^{64}CuNCs-ECL1i imaging 1 hour after transplantation, followed by a 0–10 minute dynamic scan. The relative blood flow change was evaluated by standardized uptake values (SUVs) (16).

Probe synthesis

Reagents, synthesis and characterization of all compounds are described in supporting information.

Statistical Analysis

Group variation is described as mean ± SD. Groups were compared using 1-way ANOVA with a Bonferroni post-test. Individual group differences were determined with a 2-tailed Mann–Whitney test. The significance level in all tests was $P < 0.05$. Prism, version 6.07 (GraphPad, La Jolla, CA), was used for analyses. Error bars designate standard deviation of the mean unless indicated otherwise.

Results

Recipient CCR2 expression promotes monocyte recruitment to pulmonary grafts and ischemia reperfusion injury after lung transplantation

To assess the role of recipient CCR2 expression after lung transplantation we used a model of severe ischemia reperfusion injury (13). We transplanted wildtype B6 lungs following 18 hours of cold ischemia into syngeneic wildtype or CCR2-deficient recipients. Lack of CCR2 expression in the host resulted in significant amelioration in ischemia reperfusion injury as evidenced by improvement in oxygen exchange (Figure S3A). To determine the specificity of monocyte recruitment we next transplanted B6 CD45.1 wildtype lungs into congenic B6 CD45.2 wildtype (Figure S3B) or B6 CD45.2 CCR2-deficient recipients (Figure S3C) and evaluated recipient (CD45.2) and donor (CD45.1) monocytes within the pulmonary grafts 6 hours later with flow cytometry. We noticed a substantial reduction in graft infiltration of recipient monocytes ($CD11b^{+}Ly6C^{hi}$) when the hosts lacked CCR2 expression (Figure S3D). Notably, a small population of CCR2-expressing monocytes of donor origin was present in wildtype grafts after transplantation into either wildtype or CCR2-deficient recipients. These findings were corroborated by gene expression analysis (Figure S3E). These results indicate that recipient CCR2 expression is involved in ischemia reperfusion-induced lung injury and that monocyte recruitment to the lung is CCR2-dependent in an isotype-specific manner.

Biodistribution of ^{64}Cu-DOTA-ECL1i and ^{64}CuAuNCs-ECL1i

To examine the monocyte recruitment into the lung during ischemia reperfusion injury a new CCR2 PET imaging probe (^{64}Cu-DOTA-ECL1i) was developed. The biodistribution of ^{64}Cu-DOTA-ECL1i was assessed at 1 hour after transplantation of wildtype B6 lungs into wildtype recipients. We observed high uptake in the kidneys, with minor accumulation in the liver, spleen and negligible uptake in other organs (Figure 1A), consistent with other peptide tracers (14). After transplantation of wildtype B6 lungs into wildtype B6 recipients, the uptake in the donor lung was more than twice the uptake in the native lung, consistent with the infiltration of inflammatory cells.

To further improve the imaging efficiency, multivalent ^{64}CuAuNCs-ECL1i nanoclusters with neutral surface charge and conjugated with multiple copies of ECL1i peptide were developed (Figure S4). In wildtype mice, ^{64}CuAuNCs-ECL1i demonstrated extended blood circulation at 1 hour with significant renal accumulation (Figure 1B). Consistent with a previous report from our group using ^{64}Cu nanoclusters, liver accumulation was higher compared to our findings with the monovalent probe (17). The progressive diminution in liver activity with stable uptake in the gastrointestinal tract is consistent with effective hepatobiliary excretion (17). In contrast to the decreased activity in blood pool organs observed with the peptide, the localization of the targeted nanoclusters in spleen and bone marrow remained constant throughout the 24 hour imaging period.

In vivo PET imaging of ^{64}Cu-DOTA-ECL1i peptide tracer

To assess the CCR2 imaging efficiency, ^{64}Cu-DOTA-ECL1i PET was performed in wildtype recipients of wildtype lungs. We observed uptake in the graft with minimal signal retained in

the native lung at 1 hour after transplantation (Figure 2 A, B), resulting in a graft/native lung uptake ratio of 3.71 ± 0.44. These results were indicative of infiltration of $CCR2^+$ cells into lung grafts at these time points. A PET signal was predominantly observed in B6 wildtype lungs after transplantation into CCR2-deficient recipients, consistent with donor $CCR2^+$ cells being present in these grafts at this time point. In the absence of graft infiltration of recipient $CCR2^+$ cells, the uptake in these pulmonary grafts was only 40% of that observed in wildtype lungs after transplantation into wildtype hosts. The activity of ^{64}Cu-DOTA-ECL1i retained in both lungs measured from background scans was less than 10% of the uptake acquired after the re-injection of ^{64}Cu-DOTA-ECL1i at 4 or 24 hours. Thus, the rapid clearance of this peptide tracer in lungs indicates that it can be used for serial scans in a short time period allowing for the assessment of dynamic expression of CCR2. We next wanted to assess whether differences existed between blood flow to the transplanted graft and the native lung. To this end, PET using ^{15}O-water provides a direct physiologic measurement of circulatory parameters for regional blood and vascular volume (16). PET/CT images of ^{15}O water at 1 hour after transplantation showed similar signals in both graft and native lung (Figure S5). Comparable SUV activities were observed in grafts and native lungs after transplantation of wildtype B6 lungs into syngeneic wildtype hosts, yielding a graft/native lung uptake ratio of 1.09 ± 0.28. A high intensity of PET signal in the kidney also corroborated the renal clearance determined by the biodistribution study. PET imaging performed on naïve mice showed minimal tracer uptake in the lungs (Figure S6).

The uptake in both grafts and native lungs of wildtype recipients progressively decreased at 4 and 24 hours likely reflecting temporal changes of $CCR2^+$ cell infiltration or expression of the receptor on these cells. However, the PET intensities in the pulmonary grafts were significantly higher than those in the native lungs at these later time points. The graft/native lung uptake ratio reached a peak at 4 hours (4.13 ± 0.32) and at 24 hours decreased to a level (3.73 ± 0.45) similar to that observed at 1 hour. Unlike the 63% decreased uptake in the donor lung in the wildtype B6 → wildtype B6 combination at 24 hours, we found no significant difference between the three examined time points (1, 4, and 24 hours) in wildtype lung grafts after transplantation into CCR2-deficient recipients. However, at all time points the uptake in the graft was significantly higher than in the native lung reflecting the presence of $CCR2^+$ cells that are carried over with the transplanted lung (Figure 2 A, B). When we co-injected non-radiolabeled ECL1i to block uptake of ^{64}Cu-DOTA-ECL1i, the PET signal of ^{64}Cu-DOTA-ECL1i in the grafts at 1 hour after transplantation into wildtype hosts was decreased to a level comparable to that in native lungs (Figure S7). This blocking resulted in a decrease in the graft/native lung uptake ratio, indicating binding specificity of the probe.

We have reported that ^{18}F-FDG PET can be used to detect graft rejection after pulmonary transplantation, which has been linked to glucose uptake by graft-infiltrating T cells (18). ^{18}F-FDG PET/CT showed significantly higher uptake in the donor graft than native lung at 1 hour after wildtype B6 → wildtype B6 transplantation (Figure S8). However, the FDG imaging yielded a graft/native lung uptake ratio of 2.29 ± .037, which was significantly lower than the data acquired with ^{64}Cu-DOTA-ECL1i.

In vivo PET/CT imaging of ^{64}CuAuNCs-ECL1i nanoclusters

We next set out to assess the CCR2 targeting efficiency of the multivalent ^{64}CuAuNCs-ECL1i nanoclusters. Based on the *in vivo* pharmacokinetics of ^{64}CuAuNCs-ECL1i, PET/CT images were acquired at 1, 4 and 24 hours following engraftment for both CCR2-targeted ^{64}CuAuNCs-ECL1i and non-targeted ^{64}CuAuNCs in the wildtype B6 → wildtype B6 combination. At 4 hours after transplantation, uptake of ^{64}CuAuNCs-ECL1i was observed in the grafts with minimal accumulation in the native lungs yielding a graft/native lung uptake ratio of 6.58 ± 0.47 (Figure 3). For non-targeted ^{64}CuAuNCs, the signal in the graft was significantly lower while the uptake in the native lung was comparable to the targeted counterpart, resulting in a significantly lower graft/native lung ratio (1.51 ± 0.20). Due to their small size and neutral surface charge (Figure S4), both nanoclusters were cleared through the genitourinary system, confirming the pharmacokinetic data. At 24 hours, the targeted ^{64}CuAuNCs-ECL1i nanocluster showed relatively stable uptake in both lungs while the signal was somewhat diminished in the pulmonary graft after injection of non-targeted ^{64}CuAuNCs nanoclusters. Notably, the graft/native lung ratio of ^{64}CuAuNCs-ECL1i gradually increased from 7.24 ± 0.38 at 4 hours to 8.44 ± 0.54 at 24 hours. These values were significantly higher than those obtained with the non-targeted counterpart.

Discussion

Ischemia reperfusion injury-mediated primary graft dysfunction continues to represent one of the most serious complications after lung transplantation. It does not only contribute to early morbidity and mortality, but has also been shown to be a risk factor for the development of chronic allograft dysfunction (2). Primary graft dysfunction is diagnosed and its severity graded based on the impairment of oxygen exchange and the radiographic presence of infiltrates. The identification of reliable biomarkers could facilitate a timely diagnosis of primary graft dysfunction and elucidating pathways that contribute to its pathogenesis will allow for the development of targeted therapies. We show that recruitment of CCR2$^+$ cells promotes pulmonary graft dysfunction and have used a new PET probe against CCR2 to image lung grafts during ischemia reperfusion injury. Our study demonstrates that infiltration of CCR2$^+$ cells into lung grafts can be detected noninvasively and serially using PET imaging.

Clinically, correlations exist between plasma levels of inflammatory cytokines and chemokines and the development of primary graft dysfunction in lung recipients (19, 20). MCP-1, a ligand for CCR2, has been found to be elevated in patients, who suffered from this complication. We show that recruitment of CD11b$^+$Ly6C^{hi} monocytes to pulmonary grafts is significantly reduced when recipients lack CCR2. Based on our previous observation that monocytes mediate transendothelial migration of neutrophils in injured lungs, we speculate that amelioration of ischemia reperfusion injury in CCR2-deficient recipients may in part be due to reduced neutrophilic infiltration (4). Collectively, these clinical and experimental studies indicate that CCR2 is an important contributor to ischemia reperfusion injury and therefore could serve as a biomarker of primary graft dysfunction and as a therapeutic target.

PET imaging has been used experimentally and clinically by our group and others to evaluate transplanted organs (15, 18, 21, 22). However, to date no imaging probe has been

available to detect the CCR2 receptor in vivo, which is expressed on monocytes and other cell types that are known to mediate inflammatory responses after transplantation (23, 24). We showed that a CCR2 binding peptide can specifically detect these receptors with PET/CT imaging during lung transplant-mediated ischemia reperfusion injury *in vivo* both as a monovalent peptide tracer and a multivalent nanoplatform (25). We recognize that lung stromal cells can express CCR2, which needs to be considered when interpreting CCR2 imaging results (26). However, our findings suggest that any potential contribution of such cells to the CCR2 PET signal in vivo is inconsequential compared to hematopoietic cells. As the majority of clinical pulmonary transplants are bilateral, the native lungs cannot serve as a control for the CCR2 signal in the transplanted grafts. Thus, prior to adaptation of this agent for clinical use in lung transplantation imaging of healthy volunteers will be required. This will help to establish baseline values in normal lungs that can be used to interpret signals in injured pulmonary grafts.

ECL1i has been recently demonstrated to selectively bind CCR2 in a non-competitive way compared to CCL2 ligand *in vitro* (25). In this study, ^{64}Cu-DOTA-ECL1i retention was primarily detected in the lung graft after transplantation into syngeneic CCR2-deficient recipients, consistent with the presence of donor monocytes in pulmonary grafts. Given the lack of CCR2 receptor in these hosts, we suggest that the minimal localization in native lungs was due to non-specific retention. Thus, if the localization of ^{64}Cu-DOTA-ECL1i in the native CCR2-deficient lung is due to non-specific background retention, more than 70% of the observed accumulation in the graft is due to CCR2-mediated uptake, given that ^{15}O-H_2O imaging did not show a difference in blood flow.

After lung transplantation into wildtype recipients the PET/CT images showed considerable accumulation of $CCR2^+$ cells in the whole body. Consistent with other inflammatory models we have shown that CCR2 is critical to mobilize $CD11b^+Ly6C^{high}$ monocytes from the bone marrow after lung transplantation (27, 28). In some settings CCR2 may promote monocyte recruitment from the blood into inflamed sites (29). Our imaging indicates that $CCR2^+$ cells are rapidly released into the periphery after engraftment of lungs. These observations extend previous findings where MRI imaging of myeloperoxidase activity detected graft-infiltrating Ly-$6C^{hi}$ monocytes and neutrophils during murine heart transplant rejection (30). Through competitive receptor blocking, approximately 75% of the PET signal in the grafts was blocked after transplantation into wildtype recipients, resulting in comparable retentions in both native and donor lungs. The consistent results between CCR2 receptor-specific uptake from the calculation after transplantation into CCR2-deficient hosts and the blocking percentage after engraftment into wildtype recipients support the specificity of ^{64}Cu-DOTA-ECL1i binding CCR2.

In contrast to monovalent ^{64}Cu-DOTA-ECL1i peptide tracers, we observed six-fold higher retention in the blood 1 hour after injection of targeted ^{64}CuAuNCs-ECL1i nanoclusters, confirming the advantage of multivalent nanoclusters for improved CCR2 detection (17). More importantly, the targeted ^{64}CuAuNCs-ECL1i probe demonstrated specific retention in donor grafts and minimal localization in native lungs. If the low and non-specific accumulation of ^{64}CuAuNCs in native lungs is set as background, more than 80% of the accumulation of ^{64}CuAuNCs-ECL1i in pulmonary grafts was due to CCR2-mediated

uptake, demonstrating specific and persistent imaging of CCR2. Furthermore, these specificity values were significantly higher than those for the ^{64}Cu-DOTA-ECL1i peptide tracer, underscoring the usefulness of multivalent nanoclusters for enhanced targeting and longitudinal imaging.

In conclusion, PET imaging of CCR2^{+} cells with targeted molecular probes can serve as a biomarker for primary graft dysfunction after lung transplantation. Additionally, the targeted nanoclusters provide a theranostic platform for image-guided delivery of specific treatment. These imaging approaches could be useful for a variety of CCR2-mediated inflammatory conditions, both sterile and infectious.

Supplementary Material

Refer to Web version on PubMed Central for supplementary material.

Acknowledgments

Yongjian Liu is supported by the National Institutes of Health grant R01HL125655 and Contract HHSN268201000043C (Program of Excellence in Nanotechnology). Daniel Kreisel is supported by National Institutes of Health grants 1P01AI116501, R01 HL113931, R01 HL094601 and Veterans Administration Merit Review grant 1I01BX002730.

Abbreviations

PET	positron emission tomography
SUV	standardized uptake value

References

1. Kreisel D, Krupnick AS, Puri V, Guthrie TJ, Trulock EP, Meyers BF, Patterson GA. Short- and long-term outcomes of 1000 adult lung transplant recipients at a single center. J Thorac Cardiovasc Surg. 2011; 141(1):215–22. [PubMed: 21093882]
2. Daud SA, Yusen RD, Meyers BF, Chakinala MM, Walter MJ, Aloush AA, Patterson GA, Trulock EP, Hachem RR. Impact of immediate primary lung allograft dysfunction on bronchiolitis obliterans syndrome. Am J Respir Crit Care Med. 2007; 175(5):507–13. [PubMed: 17158279]
3. Kreisel D, Sugimoto S, Zhu J, Nava R, Li W, Okazaki M, Yamamoto S, Ibrahim M, Huang HJ, Toth KA, et al. Emergency granulopoiesis promotes neutrophil-dendritic cell encounters that prevent mouse lung allograft acceptance. Blood. 2011; 118(23):6172–82. [PubMed: 21972291]
4. Kreisel D, Nava RG, Li W, Zinselmeyer BH, Wang B, Lai J, Pless R, Gelman AE, Krupnick AS, Miller MJ. In vivo two-photon imaging reveals monocyte-dependent neutrophil extravasation during pulmonary inflammation. Proc Natl Acad Sci U S A. 2010; 107(42):18073–8. [PubMed: 20923880]
5. Wang B, Zinselmeyer BH, Runnels HA, LaBranche TP, Morton PA, Kreisel D, Mack M, Nickerson-Nutter C, Allen PM, Miller MJ. In vivo imaging implicates CCR2(+) monocytes as regulators of neutrophil recruitment during arthritis. Cell Immunol. 2012; 278(1–2):103–12. [PubMed: 23121982]
6. Li L, Huang L, Sung SS, Vergis AL, Rosin DL, Rose CE Jr, Lobo PI, Okusa MD. The chemokine receptors CCR2 and CX3CR1 mediate monocyte/macrophage trafficking in kidney ischemia-reperfusion injury. Kidney Int. 2008; 74(12):1526–37. [PubMed: 18843253]
7. Liehn EA, Piccinini AM, Koenen RR, Soehnlein O, Adage T, Fatu R, Curaj A, Popescu A, Zernecke A, Kungl AJ, et al. A new monocyte chemotactic protein-1/chemokine CC motif ligand-2 competitor limiting neointima formation and myocardial ischemia/reperfusion injury in mice. J Am Coll Cardiol. 2010; 56(22):1847–57. [PubMed: 21087715]

8. Dimitrijevic OB, Stamatovic SM, Keep RF, Andjelkovic AV. Absence of the chemokine receptor CCR2 protects against cerebral ischemia/reperfusion injury in mice. Stroke. 2007; 38(4):1345–53. [PubMed: 17332467]

9. Majmudar MD, Keliher EJ, Heidt T, Leuschner F, Truelove J, Sena BF, Gorbatov R, Iwamoto Y, Dutta P, Wojtkiewicz G, et al. Monocyte-directed RNAi targeting CCR2 improves infarct healing in atherosclerosis-prone mice. Circulation. 2013; 127(20):2038–46. [PubMed: 23616627]

10. Pienta KJ, Machiels JP, Schrijvers D, Alekseev B, Shkolnik M, Crabb SJ, Li S, Seetharam S, Puchalski TA, Takimoto C, et al. Phase 2 study of carlumab (CNTO 888), a human monoclonal antibody against CC-chemokine ligand 2 (CCL2), in metastatic castration-resistant prostate cancer. Invest New Drugs. 2013; 31(3):760–8. [PubMed: 22907596]

11. Vergunst CE, Gerlag DM, Lopatinskaya L, Klareskog L, Smith MD, van den Bosch F, Dinant HJ, Lee Y, Wyant T, Jacobson EW, et al. Modulation of CCR2 in rheumatoid arthritis: a double-blind, randomized, placebo-controlled clinical trial. Arthritis Rheum. 2008; 58(7):1931–9. [PubMed: 18576354]

12. Lockhart AC, Liu Y, Dehdashti F, Laforest R, Picus J, Frye J, Trull L, Belanger S, Desai M, Mahmood S, et al. Phase 1 Evaluation of [Cu]DOTA-Patritumab to Assess Dosimetry, Apparent Receptor Occupancy, and Safety in Subjects with Advanced Solid Tumors. Mol Imaging Biol. 2015

13. Kreisel D, Sugimoto S, Tietjens J, Zhu J, Yamamoto S, Krupnick AS, Carmody RJ, Gelman AE. Bcl3 prevents acute inflammatory lung injury in mice by restraining emergency granulopoiesis. J Clin Invest. 2011; 121(1):265–76. [PubMed: 21157041]

14. Liu Y, Pierce R, Luehmann HP, Sharp TL, Welch MJ. PET imaging of chemokine receptors in vascular injury-accelerated atherosclerosis. J Nucl Med. 2013; 54(7):1135–41. [PubMed: 23658218]

15. Jones HA, Donovan T, Goddard MJ, McNeil K, Atkinson C, Clark JC, White JF, Chilvers ER. Use of 18FDG-pet to discriminate between infection and rejection in lung transplant recipients. Transplantation. 2004; 77(9):1462–4. [PubMed: 15167609]

16. Liu Y, Pressly ED, Abendschein DR, Hawker CJ, Woodard GE, Woodard PK, Welch MJ. Targeting angiogenesis using a C-type atrial natriuretic factor-conjugated nanoprobe and PET. J Nucl Med. 2011; 52(12):1956–63. [PubMed: 22049461]

17. Zhao Y, Sultan D, Detering L, Luehmann H, Liu Y. Facile synthesis, pharmacokinetic and systemic clearance evaluation, and positron emission tomography cancer imaging of (6)(4)Cu-Au alloy nanoclusters. Nanoscale. 2014; 6(22):13501–9. [PubMed: 25266128]

18. Chen DL, Wang X, Yamamoto S, Carpenter D, Engle JT, Li W, Lin X, Kreisel D, Krupnick AS, Huang HJ, et al. Increased T cell glucose uptake reflects acute rejection in lung grafts. Am J Transplant. 2013; 13(10):2540–9. [PubMed: 23927673]

19. Bharat A, Kuo E, Steward N, Aloush A, Hachem R, Trulock EP, Patterson GA, Meyers BF, Mohanakumar T. Immunological link between primary graft dysfunction and chronic lung allograft rejection. Ann Thorac Surg. 2008; 86(1):189–95. discussion 96–7. [PubMed: 18573422]

20. Hoffman SA, Wang L, Shah CV, Ahya VN, Pochettino A, Olthoff K, Shaked A, Wille K, Lama VN, Milstone A, et al. Plasma cytokines and chemokines in primary graft dysfunction post-lung transplantation. Am J Transplant. 2009; 9(2):389–96. [PubMed: 19120076]

21. Eriksson O, Eich T, Sundin A, Tibell A, Tufveson G, Andersson H, Felldin M, Foss A, Kyllonen L, Langstrom B, et al. Positron emission tomography in clinical islet transplantation. Am J Transplant. 2009; 9(12):2816–24. [PubMed: 19845588]

22. Daly KP, Dearling JL, Seto T, Dunning P, Fahey F, Packard AB, Briscoe DM. Use of [18F]FDG Positron Emission Tomography to Monitor the Development of Cardiac Allograft Rejection. Transplantation. 2015; 99(9):e132–9. [PubMed: 25675207]

23. Belperio JA, Keane MP, Burdick MD, Lynch JP 3rd, Xue YY, Berlin A, Ross DJ, Kunkel SL, Charo IF, Strieter RM. Critical role for the chemokine MCP-1/CCR2 in the pathogenesis of bronchiolitis obliterans syndrome. J Clin Invest. 2001; 108(4):547–56. [PubMed: 11518728]

24. Leuschner F, Dutta P, Gorbatov R, Novobrantseva TI, Donahoe JS, Courties G, Lee KM, Kim JI, Markmann JF, Marinelli B, et al. Therapeutic siRNA silencing in inflammatory monocytes in mice. Nat Biotechnol. 2011; 29(11):1005–10. [PubMed: 21983520]

25. Auvynet C, Baudesson de Chanville C, Dorgham K, Piesse C, Pouchy C, Carlier L, Poupel L, Felouzis V, Lacombe C, Sagan S, et al. ECL1i, d(LGTFLKC), a novel small peptide that specifically inhibits CCL2-dependent migration. The FASEB Journal. 2016

26. Tomankova T, Kriegova E, Liu M. Chemokine receptors and their therapeutic opportunities in diseased lung: far beyond leukocyte trafficking. Am J Physiol Lung Cell Mol Physiol. 2015; 308(7):L603–18. [PubMed: 25637606]

27. Gelman AE, Okazaki M, Sugimoto S, Li W, Kornfeld CG, Lai J, Richardson SB, Kreisel FH, Huang HJ, Tietjens JR, et al. CCR2 regulates monocyte recruitment as well as CD4 T1 allorecognition after lung transplantation. Am J Transplant. 2010; 10(5):1189–99. [PubMed: 20420631]

28. Serbina NV, Pamer EG. Monocyte emigration from bone marrow during bacterial infection requires signals mediated by chemokine receptor CCR2. Nat Immunol. 2006; 7(3):311–7. [PubMed: 16462739]

29. Swirski FK, Nahrendorf M, Etzrodt M, Wildgruber M, Cortez-Retamozo V, Panizzi P, Figueiredo JL, Kohler RH, Chudnovskiy A, Waterman P, et al. Identification of splenic reservoir monocytes and their deployment to inflammatory sites. Science. 2009; 325(5940):612–6. [PubMed: 19644120]

30. Swirski FK, Wildgruber M, Ueno T, Figueiredo JL, Panizzi P, Iwamoto Y, Zhang E, Stone JR, Rodriguez E, Chen JW, et al. Myeloperoxidase-rich Ly-6C+ myeloid cells infiltrate allografts and contribute to an imaging signature of organ rejection in mice. J Clin Invest. 2010; 120(7):2627–34. [PubMed: 20577051]

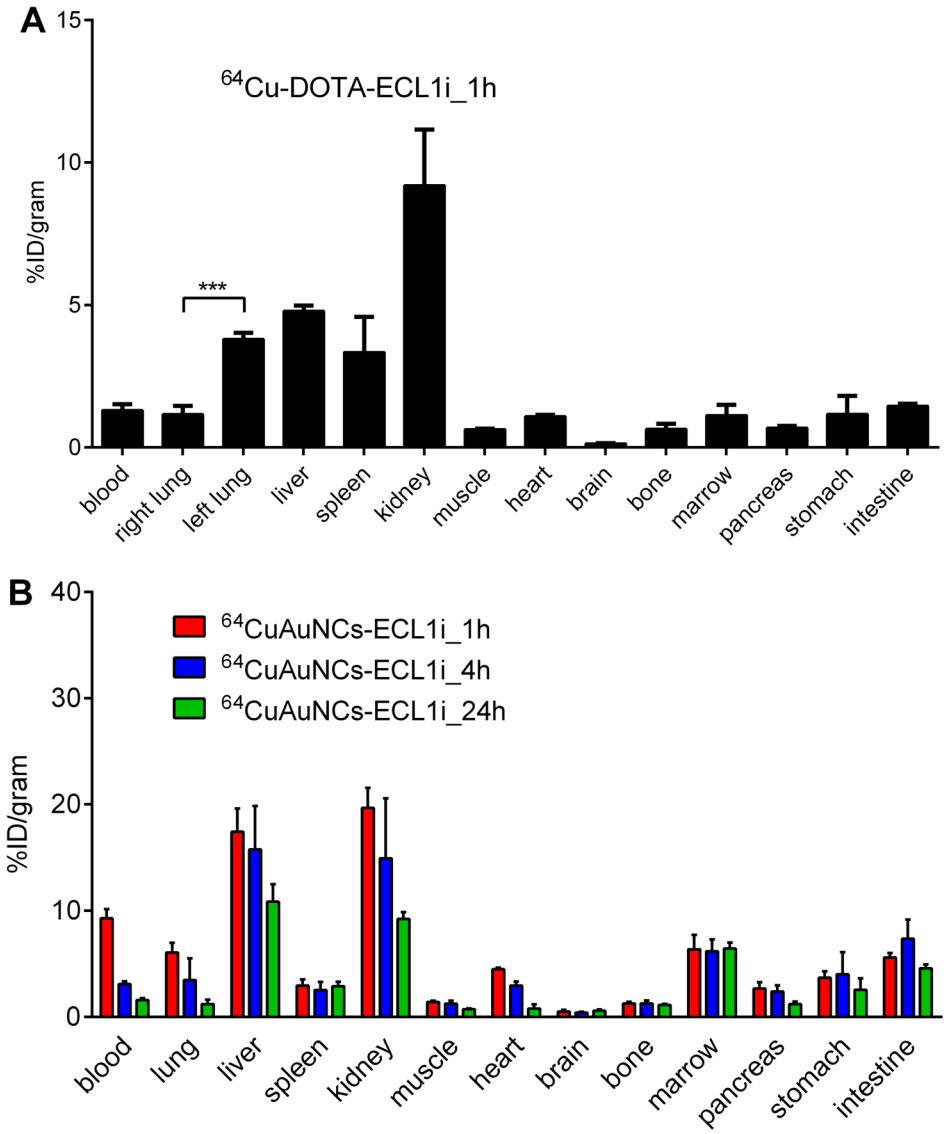

Figure 1. Biodistribution studies in B6 wildtype mice demonstrate different pharmacokinetics between ^{64}Cu-DOTA-ECL1i and ^{64}CuAuNCs-ECL1i

(A) ^{64}Cu-DOTA-ECL1i showed rapid renal clearance at 1 hour and (B) ^{64}CuAuNCs-ECL1i showed extended pharmacokinetics at 1, 4, and 24 hours (n=4/group).

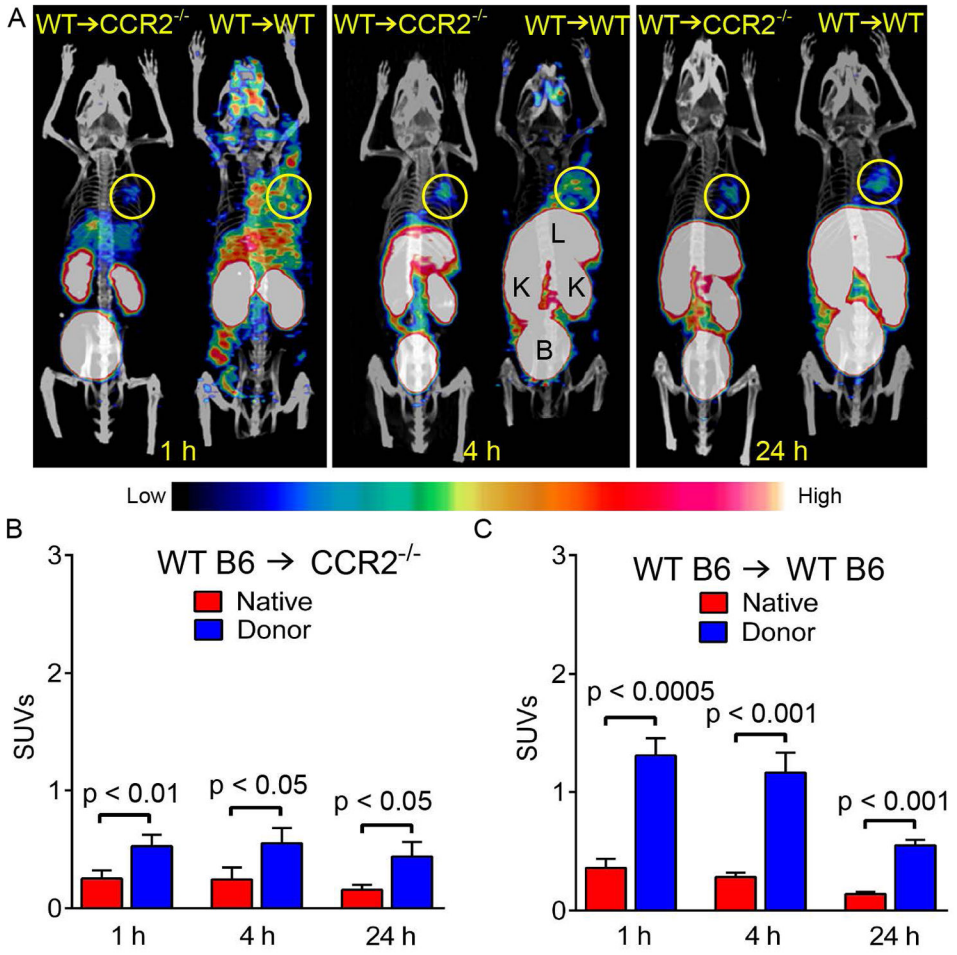

Figure 2. CCR2 is detected by ^{64}CuDOTA-ECL1i using PET

(A) Representative ^{64}CuDOTA-ECL1i PET/CT images in B6 wildtype → B6 wildtype and B6 wildtype → B6 CCR2-deficient lung transplant combinations at 1, 4 and 24 hours after transplantation. Tracer uptake was observed in the donor lungs in both models. Quantitative uptake analysis in lung grafts and native lungs after (B) B6 wildtype → B6 CCR2-deficient and (C) B6 wildtype → B6 wildtype pulmonary transplantation. L: liver, K: kidney, B: bladder. Circle: donor lung (n=4/group).

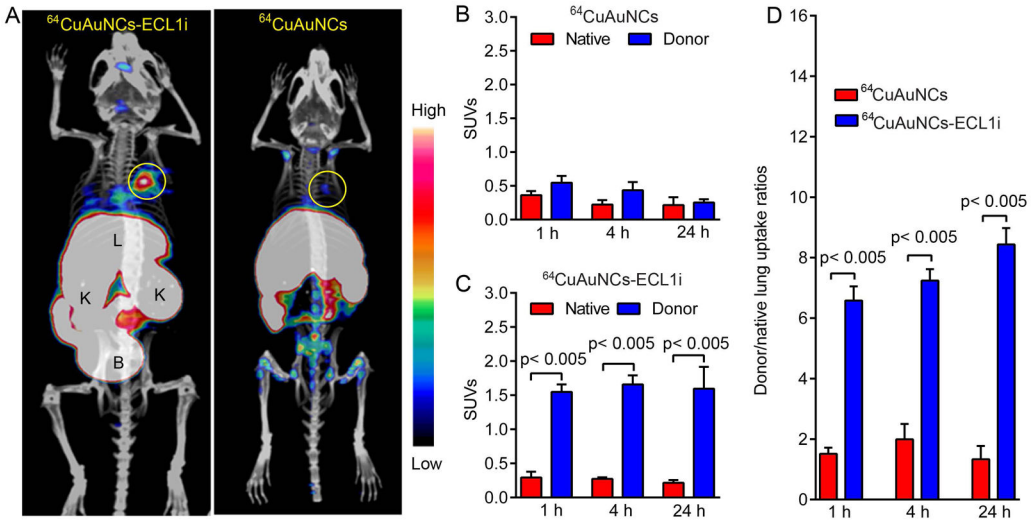

Figure 3. CCR2 is detected by ^{64}CuAuNCs-ECL1i with enhanced efficiency using PET

(A) Representative ^{64}CuAuNCs-ECL1i and ^{64}CuAuNCs nanoclusters PET/CT images in B6 wildtype → B6 wildtype lung transplantation model at 24 hours following engraftment. The targeted nanocluster showed significant uptake in the donor lung while the non-targeted counterpart showed minimum non-specific retention. Quantitative uptake analysis of (B) ^{64}CuAuNCs and (C) ^{64}CuAuNCs-ECL1i in lung grafts and native lungs after B6 wildtype → B6 wildtype pulmonary transplantation and (D) Donor graft/native lung uptake ratios for ^{64}CuAuNCs-ECL1i and ^{64}CuAuNCs PET after B6 wildtype → B6 wildtype pulmonary transplantation. Circle: donor lung (n=4/group).